

SYNAPTIC EXCITATION OF THE SECOND AND THIRD ORDER AUDITORY NEURONS IN THE AVIAN BRAIN STEM

J. T. HACKETT,¹ H. JACKSON² and E. W. RUBEL

Departments of Physiology and Otolaryngology, University of Virginia School of Medicine, Charlottesville, VA 22908, U.S.A.

Abstract—Synaptic potentials were examined in the second- and third-order auditory neurons of nucleus magnocellularis and nucleus laminaris in the chick. Brain stems of mature chick embryos were explanted and maintained *in vitro* for 4 to 8 h. Field potentials, extracellular spike potentials and intracellular potentials evoked by 8th-nerve stimulation were examined.

Eighth-nerve stimulation reliably elicited four identifiable field potentials which could be attributed to: (i) the afferent volley of the 8th-nerve axons, (ii) postsynaptic responses of n. magnocellularis neurons, and (iii) ipsilaterally and, (iv) contralaterally-evoked n. laminaris postsynaptic responses. Intracellular-recorded postsynaptic potentials from n. magnocellularis neurons were of two classes. 'Fast' excitatory postsynaptic potentials were characterized by a rapid rise time and short duration. They were apparently monosynaptic with a synaptic delay of 0.4 ms. In each n. magnocellularis neuron the 'fast' excitatory postsynaptic potentials were composed of 1 to 3 all-or-none components. 'Slow' excitatory postsynaptic potentials were characterized by a longer latency, a longer duration and graded amplitude variation in proportion to the intensity of 8th-nerve stimulation. Both 'fast' and 'slow' excitatory postsynaptic potentials had similar reversal potentials. Since the 8th nerve makes monosynaptic connection with n. magnocellularis neurons, it is likely that at this synapse the 'fast' excitatory postsynaptic potentials were produced, while the 'slow' potential may be attributable to the convergence of many bouton synapses of unknown origin.

Intracellular injections of horseradish peroxidase into n. magnocellularis revealed that its efferents bifurcate below the nucleus and send one axon to the contralateral n. laminaris while the other axon forms a highly divergent projection to the ipsilateral laminar nucleus. The intracellular records obtained from n. laminaris are consistent with this anatomical finding in that graded excitatory postsynaptic potentials were elicited by 8th-nerve stimulation.

The caliciform synaptic ending known as the end bulb of Held in the auditory nuclei is similar in both birds and mammals.²⁹ The details of transmission at these synapses have not been studied, in spite of the interest in the electrical and chemical modes of synaptic transmission in the closely related vestibular system of vertebrates^{8,9,17,18,27,31,32,45,46} and the fundamental importance of this information to the understanding of the processes of sensory integration and coding. Interestingly, for a similar calyx ending in the chick ciliary ganglion, the mode of synaptic transmission has been found to be dual—both electrical and chemical transmission coincide.²

The aim of the present investigation was to determine the modes of synaptic transmission in the first and second central nuclei of the chick auditory sys-

tem, nucleus magnocellularis (NM) and nucleus laminaris (NL) and to relate the modes of transmission to terminal morphology. The chick auditory system offers several advantages for this type of study. For example, the system has a simplified organization which is considered homologous to that found in higher vertebrates,²⁹ its development has been studied in detail^{16,33,36} and the neuronal circuit can be maintained *in vitro* to facilitate the analysis of synaptic mechanisms.

Portions of this material have been presented in two preliminary reports.^{15,34}

EXPERIMENTAL PROCEDURES

Chick embryos (Hubbard × Hubbard), just prior to hatching (18–20 days), were used for these studies. Anesthesia was effected by cooling embryos (*in ovo*) for 15 min in ice water. The cold embryo was decapitated and the head placed in cold (2°C) avian Tyrode's solution (139 mM NaCl, 3 mM KCl, 3 mM CaCl₂, 17 mM NaHCO₃, 6.4 mM glucose and gassed with 95% O₂–5% CO₂). The pH was adjusted to 7.3. The dorsal aspect of the entire skull was retracted and the brain carefully removed, making certain to leave a short length of both auditory nerves intact. The cerebellum was then removed by cutting the peduncles, and the brain stem trimmed to include the area from the obex to immediately rostral to the cerebellar peduncles.

¹ Address reprint requests to: John T. Hackett, Department of Physiology, Box 449, University of Virginia School of Medicine, Charlottesville, VA 22908, U.S.A.

² H. Jackson is now at the Department of Anatomy, University of Utah College of Medicine, Utah, U.S.A.

Abbreviations: AVCN, anteroventral cochlear nucleus; EPSP/IPSP, excitatory/inhibitory postsynaptic potential; HRP, horseradish peroxidase; MSO, medial superior olivary nucleus; NL nucleus laminaris; NM, nucleus magnocellularis.

The dissected preparation was fixed to the bottom of a specially designed chamber with cyanoacrylic glue and was allowed to warm to room temperature (21°C), while being continually superfused with oxygenated Tyrode solution at room temperature. For synaptic transmission, CaCl_2 was particularly necessary.¹¹

With the brain stem transilluminated, NM could be localized as the area under the heavily myelinated 8th-nerve fibers coursing above the nucleus (Fig. 1, between arrow heads). Bipolar stimulating electrodes were positioned on the 8th-nerve stumps as they enter the medulla or on the midline to activate the crossed dorsal cochlear tract. The intensity of stimulation was adjusted between one and two times threshold for 8th-nerve activation. Standard microelectrode recording techniques were employed. The evoked responses were recorded with micropipettes filled with either 2 M potassium citrate or a solution of 4% horseradish peroxidase (HRP) in 0.2 M KCl and 0.05 M Tris buffer.³⁹ To facilitate intracellular penetration and current injection, these two types of electrodes were beveled⁴ to resistances of 34–45 and 60–90 Mohm, respectively. Horseradish peroxidase was injected intracellularly into neurons by passing 5–8 nA outward current through the electrode for 5 min. Tissue injected with HRP was fixed by immersion in cold 4% glutaraldehyde in 0.1 M phosphate buffer for 3.5 h, then washed in buffer and allowed to sink in a solution of cold buffer and 20% sucrose. Serial frozen sections were then cut at 60 μm and reacted for HRP according to the Hanker–Yates procedure.¹²

RESULTS

The basic circuit of the avian brain stem auditory system is shown in Fig. 2A. Nucleus magnocellularis (NM) receives monosynaptic innervation from the ganglion neurons of the homolateral basilar papilla (cochlea) and is homologous to the spherical neuron region of the mammalian anteroventral cochlear nucleus (AVCN).^{1,24,29} The primary afferents form calices about the neuron bodies of NM neurons that can be easily identified at the light- and electron-microscopic level (Fig. 2B,C,D). A second type of terminal also contacts the neurons of this nucleus but its origin remains unknown (Figs 2B,C).

Neurons in nucleus laminaris (NL) form a concave monocellular lamina ventral and lateral to NM. These neurons receive binaural, tonotopic and topographically-organized innervation from NM, with spatial segregation of the ipsilateral and the contralateral innervation.^{24,35} Nucleus laminaris is usually considered homologous to the mammalian medial superior olivary nucleus (MSO).

Extracellular field potentials and single units

Figure 3A shows the field potentials evoked by single 8th-nerve stimuli that were twice threshold for ipsilateral nerve activation. There were three discernible components of this field potential: an afferent volley and two synaptic potentials (N_1 and N_2). Near the surface of NM, the shortest latency wave recorded was positive-negative-positive and probably corresponded to the compound action current generated in

the 8th nerve. The amplitude of this wave was proportional to the intensity of 8th-nerve stimulation and presumably to the number of activated 8th-nerve fibers. Furthermore, it could be recorded along the darkened path of the 8th-nerve fibers seen with transillumination. High frequency stimulation (100 Hz) did not affect the afferent volley while the longer latency, slower components decrease in amplitude. These latter components are most likely produced by synaptic currents.

With careful placement of the recording microelectrode in NM, it was possible to distinguish a small negative component, N_1 (Fig. 3A) which diminished in amplitude and eventually disappeared as the electrode was lowered through the nucleus. This is what might be expected from a cluster of neurons generating a closed field of current flow.¹³

In most recordings, the N_1 component was not distinguishable from a potential which was produced by a strong dipole field potential (N_2). Thus, there was usually a dominant sink at the surface of NM for which there is a corresponding source in depth. This type of field potential is associated with bipolar neurons in the hippocampus and cerebellum¹³ and would be expected here, given the laminar arrangement of NL neurons and an open field of current flow. The depth profile of these extracellular field potentials is plotted in Fig. 3B.

Another dipolar field potential (Fig. 4A) was recorded whose negative peak (N_3) was seen in depth. This field potential was evoked by contralateral 8th-nerve stimulation and its position corresponded to the position of the crossed dorsal cochlear tract terminals which impinge on the ventral dendrites of neurons in NL. There was a simultaneously occurring source with a peak amplitude about 250 μm from the dorsal surface. A comparison of the N_2 and N_3 waves is plotted in the depth profiles of Fig. 4B. An interpretation consistent with the above observations is that the N_1 wave is the result of a sink produced by synaptic excitation of the somas of NM neurons while the N_2 and N_3 components represent sinks produced by synaptic excitation of the dorsal and ventral dendrites of NL, respectively. The N_2 and N_3 components of the field potential, therefore, represent the convergence of the output from second- to third-order neurons.

Single neuron potentials have been recorded extracellularly from about 30 neurons. Most of these neurons were histologically identified and corroborate the evidence presented above for the structures responsible for the generation of the respective field potentials. Representative examples of single neuron potentials are shown in Fig. 5. Immediately beneath the surface, along the myelinated path of afferents, two characteristic extracellular spike potentials were recorded. One had a very short latency, following immediately after the shock artifact (Fig. 5A). This potential was usually positive going, several millivolts in amplitude, and able to follow high frequency

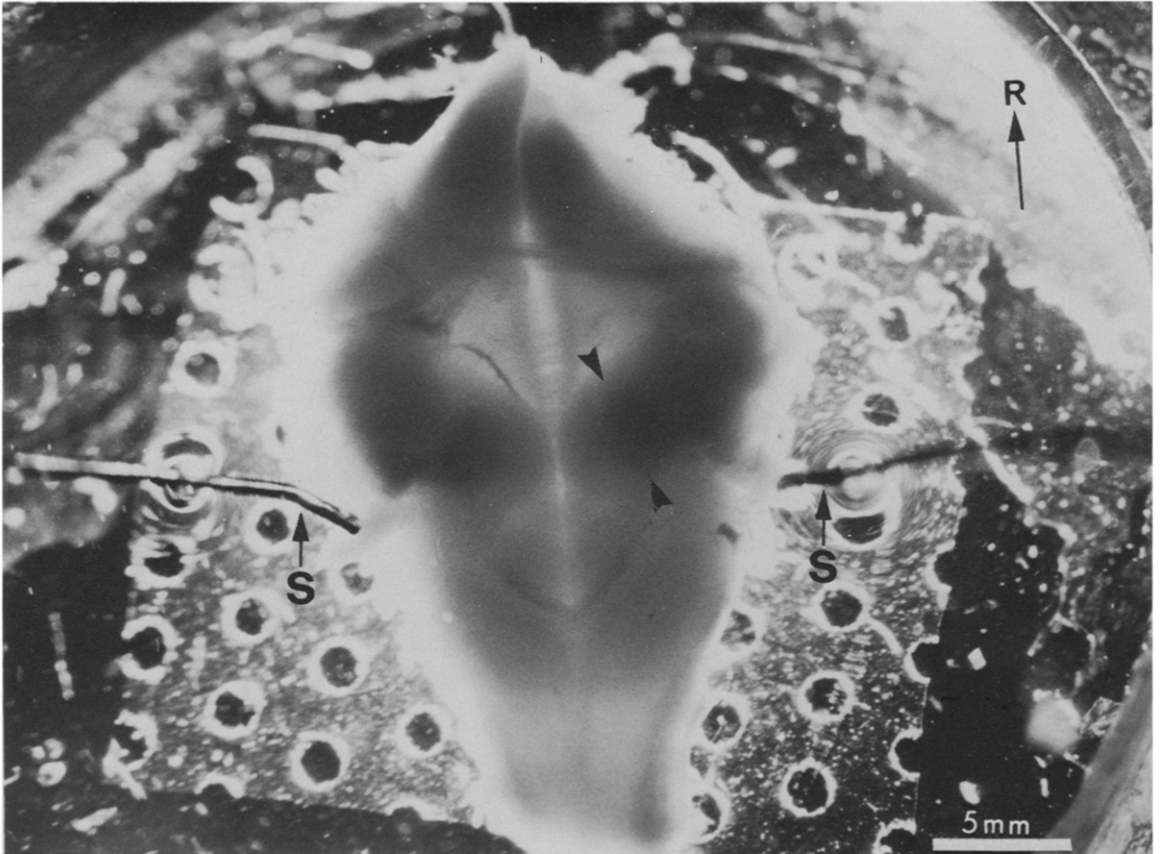


Fig. 1. Transilluminated isolated chick brain stem preparation. Dark areas (bounded by arrow heads) in floor of IVth ventricle are shadows resulting from the heavily myelinated 8th-nerve projections to n. magnocellularis. Stimulating electrodes (S) are positioned on 8th-nerve stumps. Rostral (R) indicated on orientation marker in upper right corner.

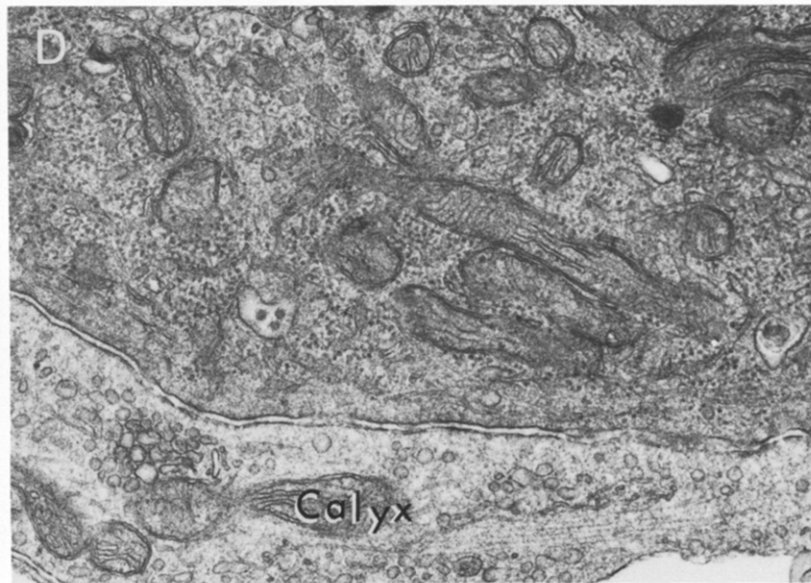
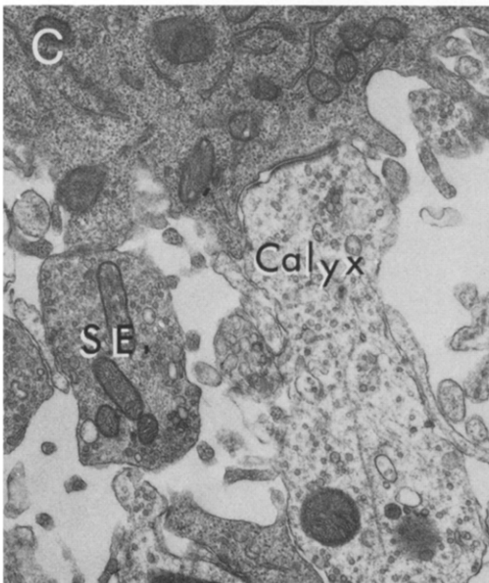
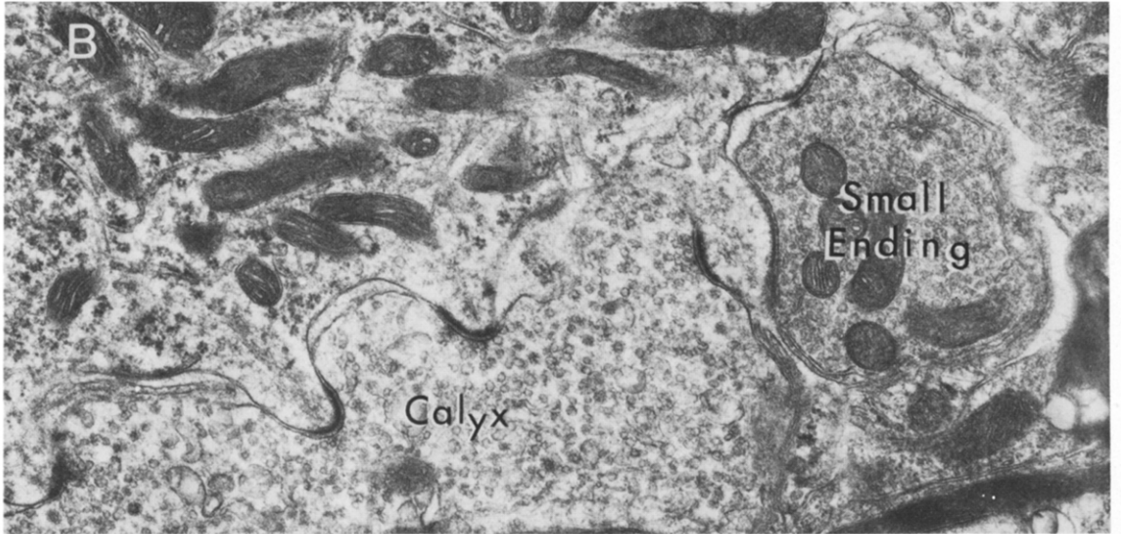
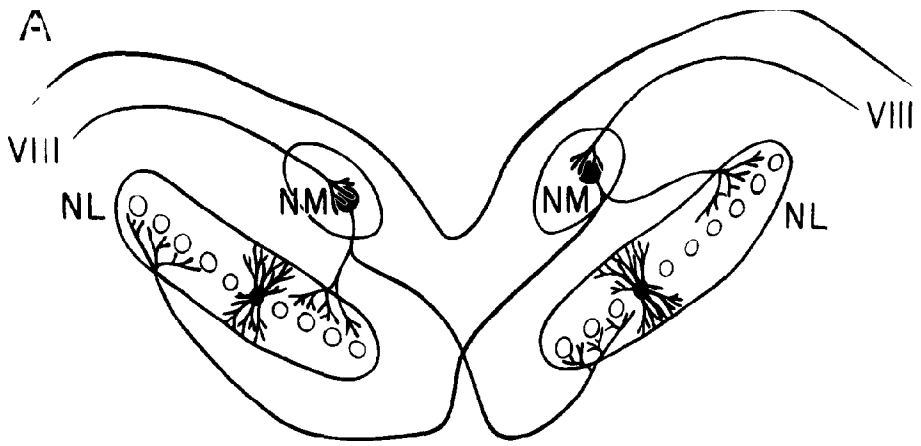


Fig. 2. Schematic representation of basic circuit of avian brain stem auditory system, showing the 8th-nerve projections from the cochlea (basilar papilla) to n. magnocellularis (NM). Note the spatially-segregated bilateral projections from NM to n. laminaris (NL). B: Electron-micrograph of section through neuron in NM showing two types of synaptic contacts. The calyx ending contains large, predominantly round clear vesicles and makes multiple, asymmetrical synaptic contacts with somatic spines of NM neuron. The small endings are packed with pleomorphic vesicles. C: Example of NM neuron with calyx and small ending (SE) from an *in vitro* experiment. D: As in C, but showing a large area of a calyx ending. Magnification: B $\times 22,400$; C $\times 16,000$; D $\times 32,000$.

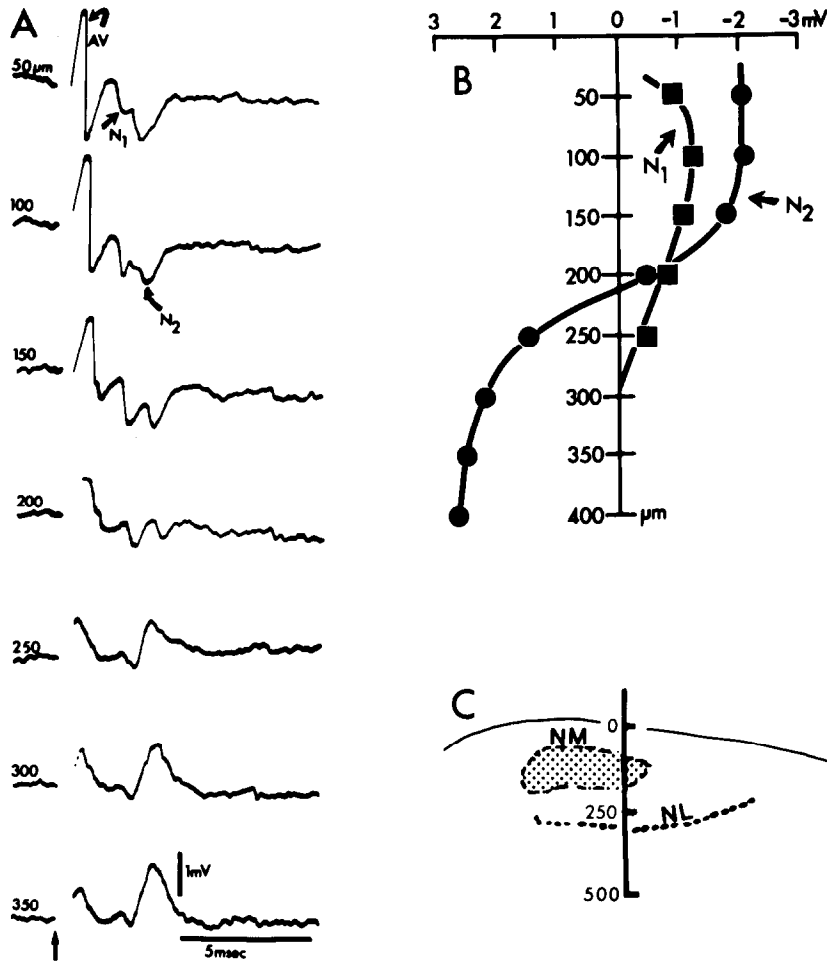


Fig. 3. Extracellular field potentials recorded at different depths of the brain stem evoked by electrical stimulation of the ipsilateral 8th nerve. A: The early positive-negative wave or afferent volley (AV) was recorded along the primary nerve pathway. The next peak negativity (N_1) is attributed to the closed field potential generated by the NM EPSPs. N_2 corresponds to the potential peak of the open current field generated by synaptic activation of NL. B: Graph showing relative amplitudes of synaptic components, N_1 (circles) and N_2 (squares), at different depths. In this and subsequent Figures, positivity at the tip of the recording microelectrode is in the upwards direction. C: Diagram showing path of electrode through NM and NL.

stimulation (100 Hz). A second characteristic unit had a delay of 3–6 ms and was blocked by calcium-free saline solution. Experimental records of spike potentials of this second sort are given in Fig. 5B,C. In Fig. 5B 2 an early notch (dot) is seen which was probably generated by the afferent volley. In particular, this small potential may reflect the invasion of action potentials into the end bulb of Held. The example illustrated in Fig. 5C 1 is similar to that in B. However, this particular example was identified as an NM neuron by antidromic activation from midline stimulation (Fig. 5C 2).

There was a third type of unit activity recorded extracellularly in these studies. This spike potential was recorded within NL as confirmed by HRP neuron marking. Neurons in NL receive afferents from both ipsilateral and contralateral NM neurons;

the ipsilateral input innervates mainly the dorsal dendrites while the ventral input impinges on the ventral dendrites (see Fig. 2A). An example of a NL unit excited by both inputs is shown in Fig. 5D. Ipsilateral activation was preceded by a small positivity that was possibly the afferent volley.

Excitatory postsynaptic potentials in nucleus magnocellularis neurons

Eighth nerve, auditory afferents terminate as the end bulb of Held in nucleus magnocellularis (NM) neurons. Stimulation of the 8th nerve resulted in spike potential generation in these neurons. In most NM neurons penetrated with a microelectrode, the membrane potential soon dropped below 40 mV and the action potential no longer contaminated the underlying synaptic potential. The relationship between the

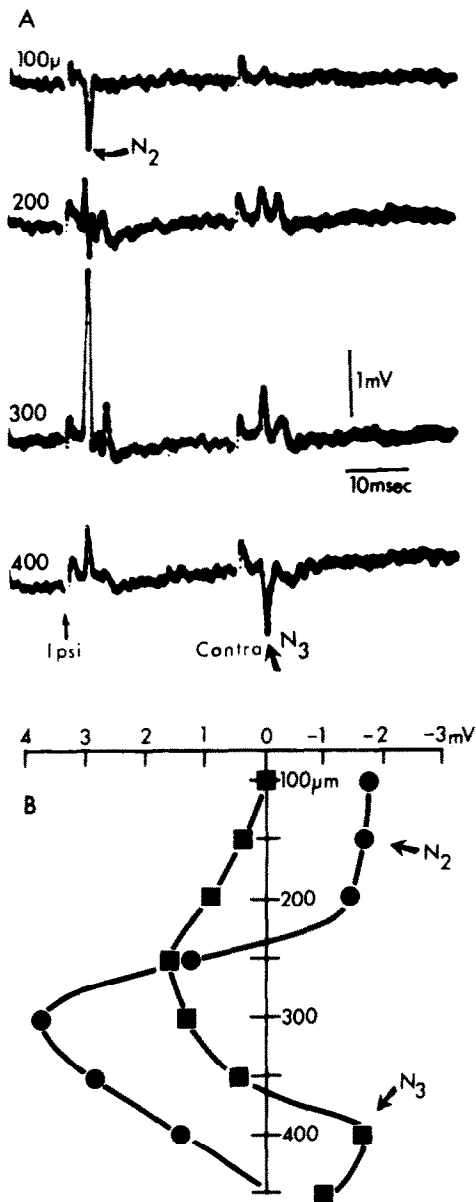


Fig. 4. A: Extracellular field potentials evoked by electrical stimuli delivered to the ipsilateral (Ipsi, first arrow) and the contralateral (Contra, second arrow) 8th nerve at each indicated electrode depth. Two stimuli were delivered for each tracing, at the times indicated by the arrows below the bottom trace. N₃ is the negative peak of the wave seen deep in the tissue evoked by contralateral nerve stimulation. Both N₂ and N₃ potentials are of the open field type. B: Graph showing relative amplitudes of synaptic components, N₂ (circles) and N₃ (squares), as a function of electrode depth.

extracellular field potential recorded just outside a NM neuron and the intracellularly-recorded EPSP is shown in Fig. 6A. An estimate of the synaptic delay was obtained assuming that the peak negativity of the afferent volley reflects the arrival of the action potentials at the terminals of 8th-nerve axons. The synaptic

delay can then be taken as the interval between the start of the action potential invasion (A1, dotted line) to the beginning of the EPSP (A2). The latter can be very accurately determined by observing the beginning of all-or-none EPSPs at threshold stimulation-intensity or by inverting the EPSPs with depolarizing current injections (Fig. 6B). The mean synaptic delay, so determined, for six neurons was $0.45 \text{ ms} \pm 0.08$ (\pm standard deviation) at 21°C. An approximate value of the synaptic delay can also be obtained from the field potentials of Fig. 3A. This was found to be 0.5 ms, a value in agreement with the above.

Another property associated with chemically-mediated synaptic transmission is depression of the postsynaptic potential following repetitive activation. Complete depression of the NM-EPSP was seen with continuous stimulation at 50 Hz (Fig. 6A 3). Also obvious in these traces is the lack of any coupling potential; only the presynaptic volley remains.

Perhaps the strongest evidence for chemically-mediated synaptic transmission comes from the demonstration of an inversion of postsynaptic potentials (e.g. see Refs 11 and 19). Inversion of NM-EPSPs was easily obtained with current injections of less than 10 nA (Fig. 6B 1). As shown in Fig. 6B 1, a progressive increase in depolarizing current injected through a balanced bridge circuit reduced and eventually inverted these EPSPs. In over 25 penetrated neurons, the reversal potential was examined at stimulus intensities that straddled threshold for 8th nerve activation or that were supra-threshold for NM-EPSPs, and no coupling potentials were ever detected. Therefore, no evidence was obtained for electrotonic transmission. The reversal of the NM-EPSPs is shown at slower sweep speed and with superimposed sweeps for each level of current injection (Fig. 6C).

In the preceding example, there was contamination of the intracellular record with a field potential probably generated by the afferent volley. The amplitude of this potential did not change upon penetration of the cell; therefore, it is unlikely that there were field effects associated with synaptic transmission. In most NM neurons studied, we did not observe the contamination of the afferent volley (Fig. 7).

Inhibitory postsynaptic potentials were not evident in these neurons. It might be argued, however, that the slower falling phase of the responses inverted by 11 nA depolarizing current injection might be due to IPSP contamination (Fig. 7A). In neurons that were hyperpolarized, there is an evident break in the falling phase (Fig. 7B, downward arrow). It has been suggested that this break is related to a voltage-dependent potassium conductance generated by the peak synaptic depolarization.¹⁹

In all neurons studied, the EPSPs in NM had one, two, or three (usually two) all-or-none components, indicating input to NM neurons from very few 8th-nerve axons. As illustrated in Fig. 7A, the responses evoked by electrical stimulation straddling threshold intensity for activation of the 8th nerve were all-or-

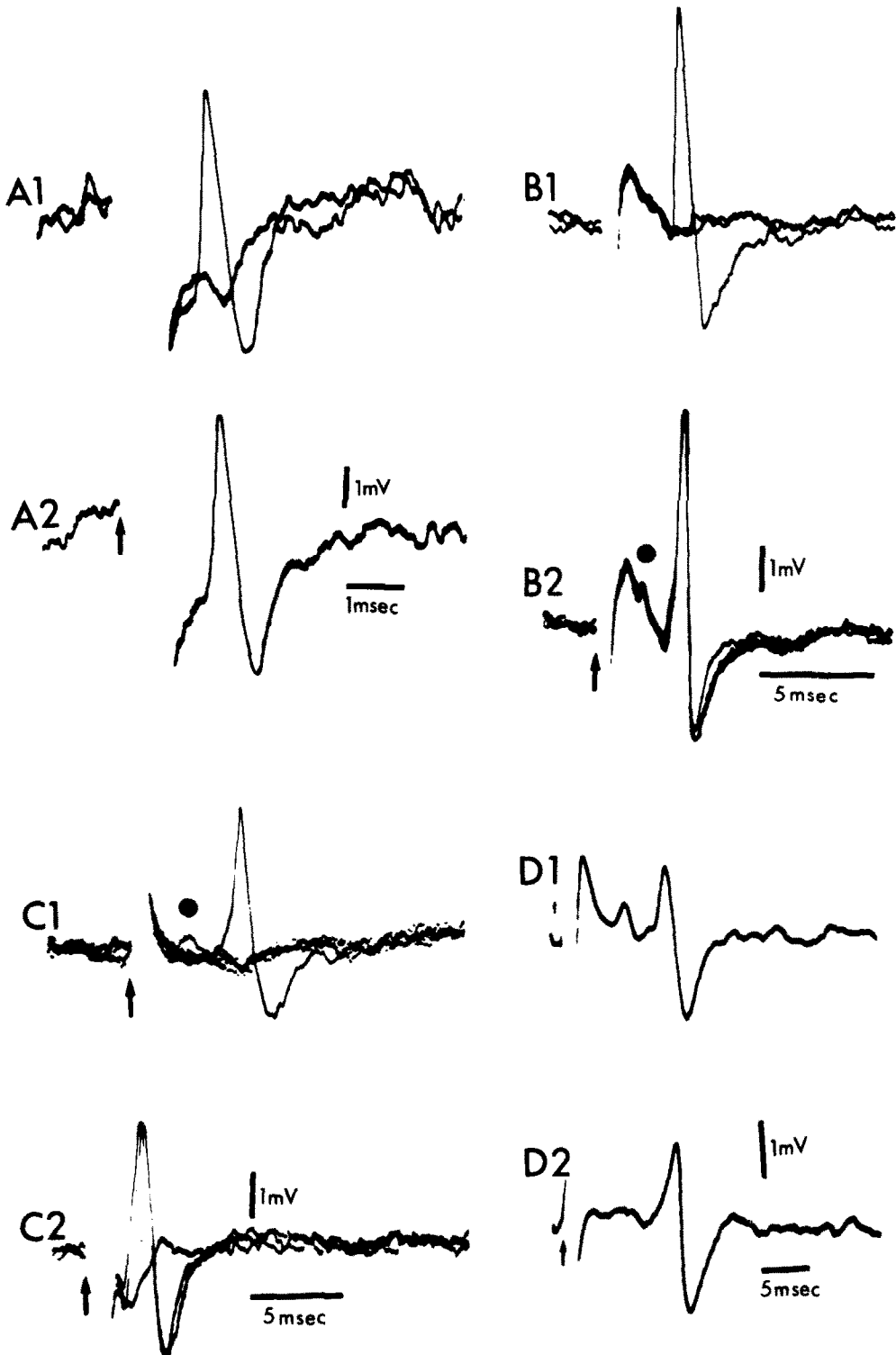


Fig. 5. Extracellular spike potentials recorded from *n. magnocellularis* and *n. laminaris* evoked by ipsilateral 8th-nerve stimulation. A: Responses from cochlear nerve fibers. B & C: Spike potentials recorded from two different NM cells. In B2 a positive notch (dot) is seen whose latency corresponds to that of the afferent volley. A similar positive potential (dot) is seen in C1 which is all-or-none and occurred coincident with the following larger spike. This unit was also fired antidromically (C2) in response to midline stimulation. D1 and D2: NL spike evoked by ipsilateral (D1) and contralateral (D2) stimuli.

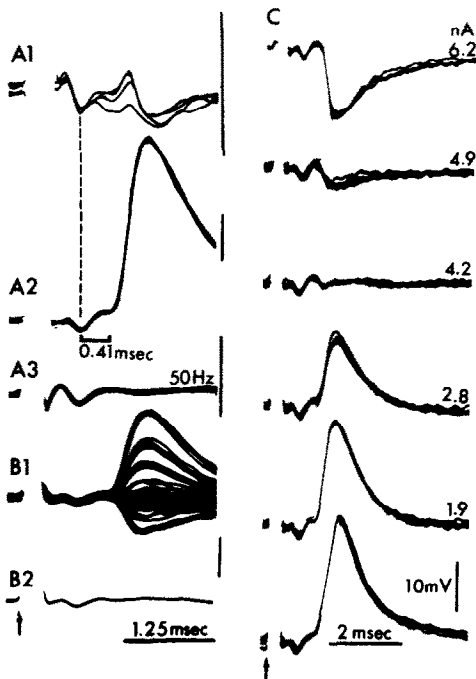


Fig. 6. Evidence for chemically-mediated synaptic transmission. Extracellular and intracellular responses in NM to ipsilateral 8th-nerve stimulation. All records from the same cell. A1, A2: Synaptic delay can be measured from the peak negativity of the extracellular afferent volley (A1, dotted line) to the beginning of the EPSP (A2, 0.41 ms). A3: At 50 Hz, repetitive stimuli produced complete depression of the EPSPs without a change in the amplitude of the afferent volley. B1: Inversion of the EPSPs by depolarizing current injection (many superimposed tracings 1.0–6.2 nA injected current). B2: Single trace at reversal potential. Note flatness of the baseline, indicating an absence of electronic coupling. C: Inversion of EPSPs as in B1, but several superimposed sweeps at the indicated amount of depolarizing current injection.

none. With increased stimulus strength (middle traces) a larger component was recruited in an all-or-nothing manner. Finally, with still higher stimulus strength, the response increases another step but no further. In Fig. 8B, another example is shown which has even larger amplitude variations in the step-increases.

We encountered two EPSP types in NM which may be related to the two types of afferent terminals which contact these neurons. The 'fast' EPSP (Figs 6, 7, 8 and 9A) has been seen in every NM neuron penetrated. It has a rapid rise time, short duration and reliably follows the stimulus train in a one-to-one fashion. The second type of postsynaptic potential recorded from NM neurons was characterized by a slow time course (Fig. 9A) and a graded amplitude (Fig. 9B) and a longer latency than the 'fast' EPSPs. This 'slow' EPSP was always depolarizing except when reversed by depolarizing current injections. The reversal potentials for both 'fast' and 'slow' EPSPs

were about the same (Fig. 9C). This 'slow' potential was not reliably elicited by 8th-nerve stimulation and did not faithfully follow the stimulus train. The duration of the 'slow' potential was about 50 ms. Two characteristics of this postsynaptic potential have a bearing on the nature of NM neuron innervation. First, in response to 8th nerve stimulation the latency of the 'slow' EPSPs was always longer than the 'fast' EPSPs (Fig. 9A). It is, therefore, likely that the latter are the result of primary afferent activation. Secondly, the graded amplitude of the 'slow' EPSP indicates that there are many afferents (always greater than five) contributing to this potential. Since there are many small axons converging on a NM neuron, it is likely that they produce the 'slow' EPSP. Although the neurons of origin of these axons have not yet been identified, the anatomical observation of recurrent collaterals from NM neurons coursing back through the nucleus suggests the possibility that the 'slow' EPSP results from NM neurons terminating on one another. There are, of course, many other plausible explanations, including local circuits within the brain stem, or a second class of 8th-nerve axons.⁴⁴

Inhibitory postsynaptic potentials in nucleus magnocellularis neurons

In all neurons which were not depolarized by current injections, there was no evidence of hyperpolarizing potentials. However, following repetitive stimulation (about 10 Hz) or while recording from neurons which were strongly depolarized, there was occasionally an increase in the falling phase of the inverted EPSP or the appearance of a hyperpolarizing potential while the first portion of the EPSP was still in the depolarizing direction. When KCl-filled microelectrodes were used (see Experimental Procedures), there was no change in the amplitude of postsynaptic potentials which could be attributed to a leak of chloride ion into the neurons. Similarly, no evidence for IPSPs in vestibular neurons has been reported.^{18,27} These results are somewhat surprising since both Gray type I and type II synapses were observed on NM neurons and in the lateral vestibular nucleus of the toadfish.¹⁸

Postsynaptic potentials in nucleus laminaris neurons

Figure 10 shows intracellularly-recorded EPSPs from an NL neuron in response to ipsilateral 8th-nerve stimulation. The amplitude of the EPSPs increased in proportion to the intensity of 8th nerve stimulation (Fig. 10A) and with hyperpolarizing current injections into NL neurons. Excitatory postsynaptic potentials decreased with depolarizing current injections and with strong depolarization were inverted (Fig. 10B). Inhibitory postsynaptic potentials were not obvious in our records. The composite character of the EPSP, and especially the small components seen, suggests that many NM axons converge onto each NL neuron.

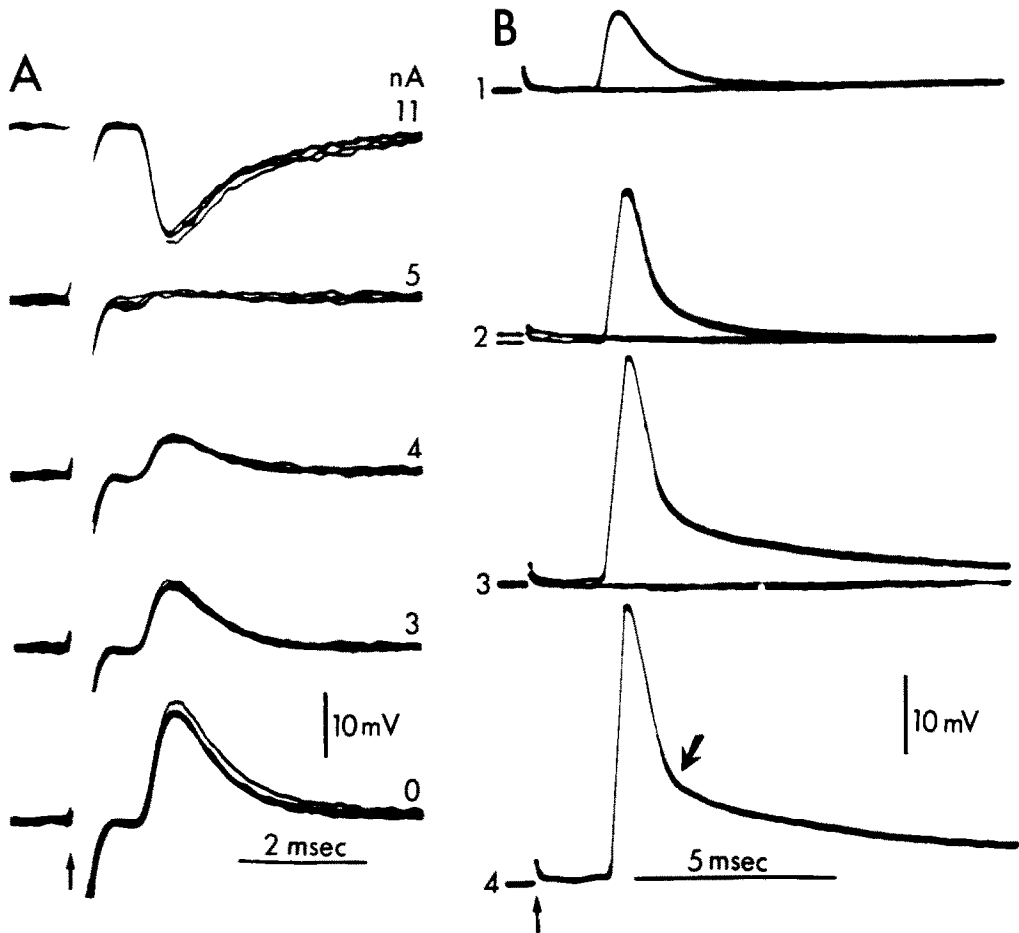


Fig. 7. A: Inversion of excitatory postsynaptic potential recorded in NM neuron as in Fig. 6C but in the absence of preceding negative field potential. B: the falling phase of the EPSPs has two parts which become more evident during hyperpolarization. (1-4, increasing current injection) Note the all-or-none EPSPs.

Morphology of nucleus magnocellularis terminals in nucleus laminaris

By intracellular labeling of NM neurons with HRP, it is possible to examine the course of NM axons and their terminal distribution in NL. One example is shown in Fig. 11. An individual NM neuron was penetrated, characterized electrophysiologically and then injected with HRP. About 1.5 h later, the tissue was fixed and processed to reveal the morphology of the penetrated neuron. Figure 11A shows a composite tracing from serial sections through the ipsilateral NM and NL. A single HRP-marked axon coursed ventrally and slightly posteriorly; it then bifurcated, and one branch crossed the midline. The other branch turned back to run dorsolaterally through NM at the level of its neuron body. This branch then traveled rostrally for 250–300 μm . At this point, the fiber dropped ventromedially to NL in a cascade of bifurcations which resulted in an elaborate terminal arbor. This figure demonstrates the divergence of projections

from an individual NM neuron onto 25–35 adjacent neurons in NL.

DISCUSSION

Extracellular potentials from auditory nuclei

Each element of the scheme in Fig. 2A can be correlated with an extra-culturally-recorded field potential. The afferent volley was recorded first in time and was largest in amplitude in the tract of 8th-nerve fibers that course over the auditory nuclei. The volley had the characteristic, positive-negative-positive wave of a compound action current propagated in a volume conductor.¹³ Recording of units in NM revealed a small positive notch in the evoked response which may be related to the calyx ending of the 8th-nerve afferents. However, this potential is not as prominent as those seen in the records from the mammalian cochlear nucleus²⁶ or in the turtle cerebellum.⁴³

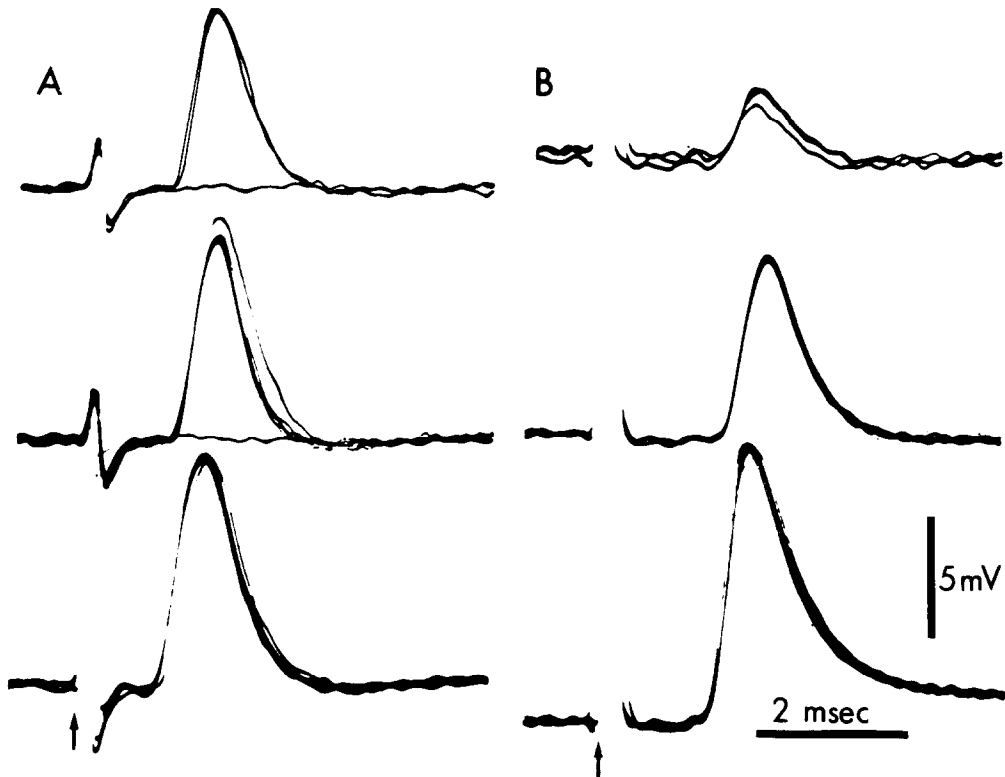


Fig. 8. All-or-none property of excitatory postsynaptic potential. A: Synaptic potentials evoked by increasing intensities of stimuli delivered to the 8th nerve. Note that the smallest response, in response to stimulation which straddled threshold for activation of 8th nerve (top), is all-or-none. Similarly, with high stimulus strengths, the amplitude of the EPSPs increase but in a step-wise fashion. Further increase in stimulus strength did not recruit more than these three units (bottom). B: Another cell showing wider fluctuations in unit increments of EPSP amplitude. Only three steps were evident.

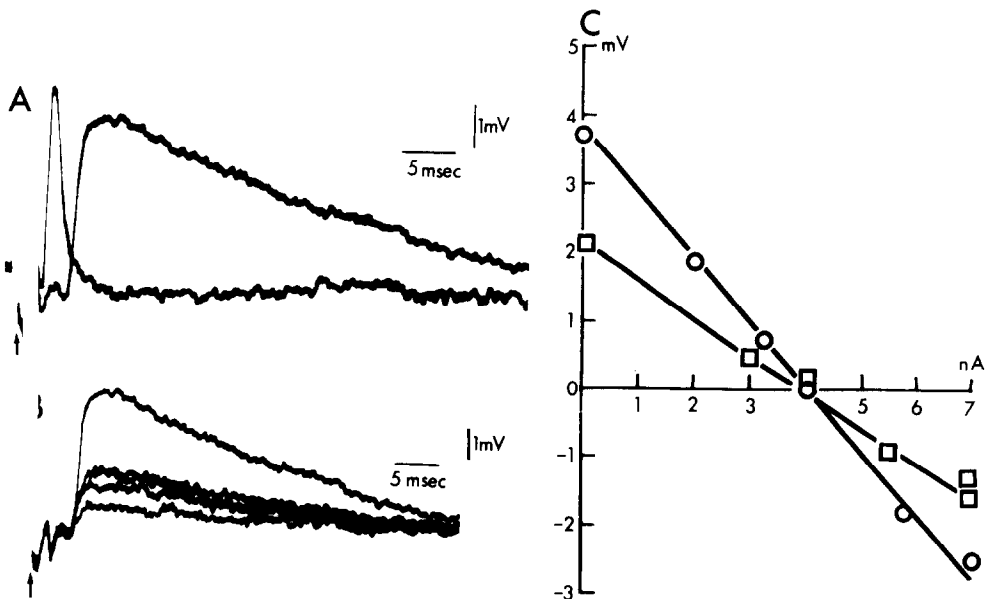


Fig. 9. A: 'Fast' and 'slow' excitatory postsynaptic potentials recorded from the same nucleus magnocellularis neuron. Note differences in latency and time course of these two potentials. B: 'Slow' EPSP from NM cell with graded amplitude proportional to the intensity of 8th-nerve stimulation. C: Plot of synaptic potential amplitude (circles: 'fast' EPSP, squares: 'slow' EPSP) as a function of depolarizing current injection.

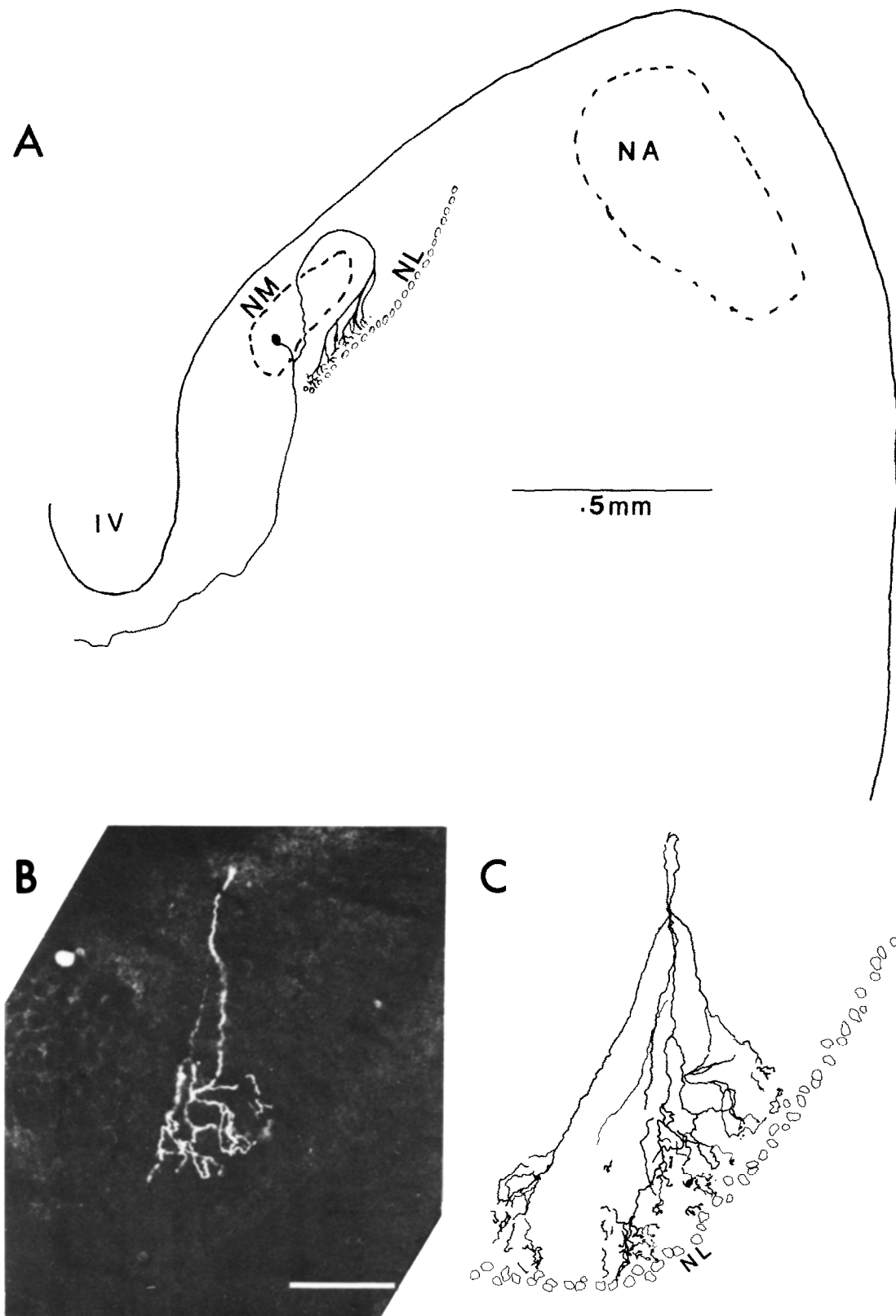


Fig. 11. Intracellular staining of a single nucleus magnocellularis cell. A: Reconstruction from serial tracings of brain sections in which a single NM cell was injected with HRP. Note course of ipsilateral collateral from NM to NL. B: Dark-field photomicrograph showing terminal field seen in one section. Bar = 100 μ m. C: Reconstruction of terminal field of this cell in the ipsilateral NL from 3 adjacent sections, one of which is shown in B.



Fig. 10. Excitatory postsynaptic potentials recorded in nucleus laminaris evoked by ipsilateral 8th-nerve stimulation. A: The irregular shape and multiple components indicate that this potential is produced in response to the activation of many converging afferent terminals. These EPSPs summate as the intensity of stimulation increases (1–3). B: The EPSPs were inverted by depolarizing current injections.

Following the afferent volley are two synaptic field potentials. The earliest is restricted to NM and is of the closed-field type. The second can be recorded over several hundred microns and is a typical dipole field that is most likely generated by synaptic activation of NL.

Relation of excitatory postsynaptic potentials to terminals in nucleus magnocellularis

Horseradish peroxidase-labeling of nerve terminals in NM has revealed large caliciform terminals encompassing as much as one-third of individual cell somas.²⁵ These endings were also identified in electron-micrographs of NM from normal animals^{16,46} (Fig. 2B) and from tissue which has been recorded from *in vitro* (Fig. 2C). As shown in Fig. 2, these terminals form synaptic specializations on somatic spines as well as smooth somatic membrane. Stimulation of the 8th nerve evoked powerful excitation of NM cells which was consistent with the large size and close proximity of these synapses to the NM cell soma. The presence of two or three all-or-none components of these EPSPs indicates that there is a corresponding number of afferents innervating the postsynaptic cell. This is consistent with early Golgi studies²⁹ and more recent electron-microscopic studies.¹⁶ Thus,

anatomical studies (Golgi, electron-microscopic and HRP) support the contention that the end bulbs of Held are responsible for the powerful and direct excitation of NM. In addition, this interpretation is consistent with cell-counting studies performed in our laboratory. Nucleus magnocellularis is composed of approximately 4500 neurons^{23,36} while there are 12,000–14,000 cochlear ganglion cells in the chick (S. R. Young & E. W. Rubel, unpublished observations). Thus, it would appear that there is a convergence ratio of 2 or 3:1 and little or no divergence in the 8th-nerve innervation of NM.

The second type of terminal found on NM cells was bouton in shape, did not contact somatic spines, had only one or two synaptic specializations per bouton and had vesicles much more densely packed than those found in the end bulbs described above (Figs 2B and C). Golgi impregnations¹⁶ reveal that a single axon may issue bouton terminals to many NM cells and that a single NM cell receives bouton endings from many converging axons. It is likely that these bouton endings are responsible for the graded, 'slow' EPSP described above. The cell bodies of these afferents have not been identified.

Mode of transmission in auditory nuclei compared with vestibular nuclei

Synaptic transmission from primary afferent vestibular fibers to vestibular neurons has been extensively investigated in recent years. Much of this interest has been generated by the demonstration of electrotonic transmission and the possibility of dual electrotonic and chemical transmission.^{8,9,17,18,27,31,32,45,46} In the auditory nuclei, no evidence for electrotonic transmission has been forthcoming. On the contrary, Pfeiffer²⁶ suggested, on the basis of delay between pre- and post-synaptic spike potentials, that transmission between primary auditory afferents and cells of the AVCN. In Fig. 6, we have presented clear evidence for chemically-mediated synaptic transmission. Furthermore, synaptic potentials were inverted by depolarizing current injections with no evidence of electrotonic coupling and postsynaptic potentials were reversibly eliminated by a calcium-free superfusate. There were no potentials that could be attributed to coupling between postsynaptic cells. In contrast, there are occasional gap junctions between cochlear nuclear cells in the rat.⁴⁰ In light of this finding, it would be of interest to examine electrophysiologically the question of electrotonic transmission in mammals.

Intracellular recordings from mammalian cochlear nucleus

Since one of the objectives of our experiments was to provide additional information on the synaptic events which may be occurring in the AVCN and MSO of mammals (through the proposed homologies with NM and NL), a brief description of what is known regarding intracellular events in these mam-

malian nuclei is relevant. There have been a number of studies of intracellular potentials in the mammalian cochlear nucleus;^{2,3,6,7,10,30,41,42} we know of no intracellular investigations of MSO neurons. The studies of the AVCN have used pure-tone or click stimuli and are primarily attempts to determine the synaptic events responsible for the extracellular-response-pattern classification.²⁶ The results of these studies were interpreted in terms of afferents activated by different types of acoustic stimuli without regard to further identification of these afferents. We have, in contrast, found two types of EPSPs which can be related to the caliciform and bouton endings that contact the NM cells. We suspect that similar synaptic potentials will be found in the mammalian AVCN as the caliciform and small bouton terminal-types have also been identified in that nucleus.^{5,14,20,21,38}

There is strong, but indirect, evidence that 'primary-like' responses in AVCN are recorded from postsynaptic cells which receive the end bulbs of Held.²⁶ The findings in the present study that the 'fast' EPSP in NM follows nerve stimulation in a one-to-one fashion further reinforces this conclusion. On the other hand, the synaptic mechanisms responsible for the inhibition of activity following tone-evoked discharges are not clear, although we did find a suggestion of a hyperpolarizing potential which could be responsible for tone-evoked suppression of activity. The observations on mammalian cells with more complex response patterns are not relevant since only 'primary-like' responses with some inhibitory surrounds at

higher stimulus intensities have been identified in NM.^{35,37}

Maturation changes in electrophysiological characteristics of nucleus magno-cellularis and nucleus laminaris

The present results were obtained from near-term embryos and although the major developmental events have occurred by this age,³³ several developmental changes which might be expected to affect the electrophysiology of this system had not been completed in these subjects. Given the several examples of developmental synapse elimination documented within both the peripheral and central nervous system,²⁸ it is reasonable to assume that the number of afferents converging on a given postsynaptic target cell is to some extent age-dependent. We have found NM neurons to be innervated by only 1-3 8th-nerve fibers, so this number could not be much reduced at a later stage of development. However, the possibility of subsequent reductions in the degree of divergence by NM axons and their convergence on individual NL targets remains.

Acknowledgements—The authors wish to thank Mrs B. Ferguson for careful typing and Ms P. Palmer for histological assistance. Support was provided by NSF grant BNS 04074, NIH PHS grant NS15478, funds from the Deafness Research Foundation, and RCDA NS000305 to E.W.R.; NSF grant BNS 155271 and NIDA RSDA 0009 to J.T.H., and NIH Program Project grant NS14620.

REFERENCES

- Boord R. L. (1969) The anatomy of the avian auditory system. *Ann. N.Y. Acad. Sci.* **167**, 186-198.
- Britt R. & Starr A. (1976a) Synaptic events and discharge patterns of cochlear nucleus cells—I. Steady-frequency tone bursts. *J. Neurophysiol.* **39**, 162-178.
- Britt R. & Starr A. (1976b) Synaptic events and discharge patterns of cochlear nucleus cells—II. Frequency-modulated tones. *J. Neurophysiol.* **39**, 179-194.
- Brown K. T. & Flaming D. G. (1975) Beveling of fine micropipette electrodes by a rapid precision method. *Science N.Y.* **185**, 693-695.
- Cant N. B. & Morest D. K. (1979) The bushy cells in the anteroventral cochlear nucleus of the cat. A study with the electron-microscope. *Neuroscience* **4**, 1925-1945.
- Caspary D. (1972) Classification of subpopulations of neurons in the cochlear nucleus of the kangaroo rat. *Expl Neurol.* **37**, 131-151.
- Erulkar S. D., Butler R. A. & Gerstein G. L. (1968) Excitation and inhibition in cochlear nucleus—II. Frequency-modulated tones. *J. Neurophysiol.* **31**, 537-548.
- Faber D. S., Kaars C. & Zottoli S. J. (1980) Dual transmission at morphologically mixed synapses: evidence from postsynaptic cobalt injections. *Neuroscience* **5**, 433-440.
- Furshpan E. J. (1964) 'Electrical transmission' at an excitatory synapse in a vertebrate brain. *Science, N.Y.* **144**, 878-880.
- Gerstein F. L., Butler R. A. & Erulkar S. D. (1968) Excitation and inhibition in cochlear nucleus—I. Tone-burst stimulation. *J. Neurophysiol.* **31**, 526-536.
- Hackett J. T. (1976) Calcium-dependence of excitatory chemical synaptic transmission in the frog cerebellum *in vitro*. *Brain Res.* **114**, 35-46.
- Hanker J. S., Yates P. E., Metz C. B. & Rustioni A. (1977) A new specific, sensitive and non-carcinogenic reagent for the demonstration of horseradish peroxidase. *Histochem. J.* **9**, 789-792.
- Hubbard J. I., Llinás R. & Quastel D. M. J. (1969) *Electro-physiological Analysis of Synaptic Transmission* pp. 275-279. Williams and Wilkins Co., Baltimore.
- Ibata Y. & Pappas G. D. (1976) The fine structure of synapses in relation to the large spherical neurons in the anterior ventral cochlear nucleus of the cat. *J. Neurocytol.* **5**, 395-406.

15. Jackson H., Hackett J. T. & Rubel E. W. (1978) *In vitro* electro-physiological analysis of N. magnocellularis and N. laminaris of the chicken. *Soc. Neurosci. Abs.* **2**, 1005.
16. Jhaveri S. T. (1978) Morphogenesis in the auditory system of the chicken: a study of nucleus magnocellularis. Doctoral dissertation, Harvard Univ.
17. Korn H., Crepel F. & Sotelo C. (1973) Electrotonic coupling between neurons in the rat vestibular nucleus. *Expl Brain Res.* **16**, 255–275.
18. Korn H., Sotelo C. & Bennett M. V. L. (1977) The lateral vestibular nucleus of the toadfish *Opsanus tau*: ultrastructural and electrophysiological observations with special reference to electrotonic transmission. *Neuroscience* **2**, 851–884.
19. Llinás R. & Nicholson C. (1976) Reversal properties of climbing fiber potential in cat Purkinje cells: an example of a distributed synapse. *J. Neurophysiol.* **39**, 311–323.
20. Lorente de Nó R. (1976) Some unresolved problems concerning the cochlear nerve. *Ann. Otol. Rhinol. Lar. Suppl.* **34**, 85, 1–28.
21. McDonald D. M. & Rasmussen G. L. (1971) Ultrastructural characteristics of synaptic endings in the cochlear nucleus having acetylcholinesterase activity. *Brain Res.* **28**, 1–18.
22. Martin A. R. & Pilar G. (1963) Dual mode of synaptic transmission in the avian ciliary ganglion. *J. Physiol.* **168**, 443–463.
23. Parks T. N. (1979) Afferent influences on the development of the brain stem auditory nuclei of the chicken: otocyst ablation. *J. comp. Neurol.* **183**, 665–678.
24. Parks T. N. & Rubel E. W. (1975) Organization and development of brain stem auditory nuclei of the chicken: organization of projections from n. magnocellularis to n. laminaris. *J. comp. Neurol.* **164**, 435–448.
25. Parks T. N. & Rubel E. W. (1978) Organization and development of the brain stem auditory nuclei of the chicken: primary afferent projections. *J. comp. Neurol.* **180**, 439–448.
26. Pfeiffer R. P. (1966) Anteroventral cochlear nucleus: wave forms of extracellularly-recorded spike potentials. *Science, N.Y.* **154**, 667–668.
27. Precht W., Richter A., Ozawa S. & Shimazu H. (1974) Intracellular study of frog's vestibular neurons in relation to the labyrinth and spinal cord. *Expl Brain Res.* **19**, 377–393.
28. Purves D. & Lichtman J. W. (1980) Elimination of synapses in the developing neurons system. *Science, N.Y.* **210**, 153–157.
29. Ramón Y Cajal S. (1908) Les ganglions terminaux du nerf acoustique des oiseaux. *Trab. Inst. Cajal Invest. Biol.* **6**, 195–225.
30. Ramond R. (1978) Survey of intracellular recording in cochlear nucleus of the cat. *Brain Res.* **148**, 43–65.
31. Richter A., Precht W. & Ozawa S. (1975) Responses of neurons of lizard's *Lacerta viridis*, vestibular nuclei to electrical stimulation of the ipsi- and contralateral VIIIth nerves. *Pflugers Arch. ges. Physiol.* **355**, 85–94.
32. Rovainen C. M. (1979) Electrophysiology of vestibulospinal and vestibuloreticulospinal systems in lampreys. *J. Neurophysiol.* **42**, 745–766.
33. Rubel E. W. (1978) Ontogeny of structure and function in the vertebrate auditory system. In *Handbook of Sensory Physiology* (ed. Jacobson M.) Vol. 9, pp. 135–237. Springer-Verlag, New York.
34. Rubel E. W., Jackson H. & Hackett J. T. (1978) *In vitro* analysis of synaptic potentials and neuronal morphology in avian brain stem auditory nuclei. *J. acoust. Soc. Am.* **64**, Suppl. 1, 386.
35. Rubel E. W. & Parks T. N. (1975) Organization and development of the brain stem auditory nuclei of the chicken: tonotopic organization of n. magnocellularis and n. laminaris. *J. comp. Neurol.* **164**, 411–434.
36. Rubel E. W., Smith D. J. & Miller L. C. (1976) Organization and development of brain stem auditory nuclei of the chicken: ontogeny of n. magnocellularis and n. laminaris. *J. comp. Neurol.* **166**, 469–489.
37. Sachs M. B. & Sinnott J. M. (1978) Responses to tones of single cells in nucleus magnocellularis and nucleus angularis of the redwing blackbird (*Agelaius phoeniceus*). *J. comp. Physiol.* **126**, 347–361.
38. Schwartz A. M. & Gulley R. L. (1978) Non-primary afferents to the principal cells of the rostral anteroventral cochlear nucleus of the guinea-pig. *J. comp. Physiol.* **153**, 489–508.
39. Snow P. J., Rose P. K. & Brown A. G. (1976) Tracing axons and axon collaterals of spinal neurons using intracellular injection of horseradish peroxidase. *Science, N.Y.* **191**, 312–313.
40. Sotelo C., Gentschev T. & Zamora A. J. (1976) Gap junctions in ventral cochlear nucleus of the rat. A possible new example of electrotonic junctions in the mammalian C.N.S. *Neuroscience* **1**, 5–7.
41. Starr A. & Britt R. (1970) Intracellular recordings from cat cochlear nucleus during tone stimulation. *J. Neurophysiol.* **33**, 137–147.
42. Starr A. & Britt R. (1972) Synaptic events in cochlear nucleus. In *Physiology of the Auditory System* (ed. Sachs M. B.) pp. 175–188. Natl. Educ. Consultants, Baltimore.
43. Walsh J. V., Houk J. C. & Mugnaini E. (1974) Identification of unitary potentials in turtle cerebellum and correlations with structures in granular layer. *J. Neurophysiol.* **37**, 30–47.
44. Whitehead M. C. & Morest D. K. (1981) Dual populations of efferent and afferent cochlear axons in the chicken. *Neuroscience* **6**, 2351–2365.
45. Wilson V. J. & Wylie R. M. (1970) A short-latency labyrinthine input to the vestibular nuclei in the pigeon. *Science, N.Y.* **168**, 124–126.
46. Wylie R. M. (1973) Evidence of electrotonic transmission in the vestibular nuclei of the rat. *Brain Res.* **50**, 179–183.